**ROSE/TN/2002-02** to be published in an abridged form in NIMA

# Study of the frequency and temperature dependence of the depletion voltage from CV measurements for irradiated Si detectors

D.Campbell, A.Chilingarov*, T.Sloan
Department of Physics, Lancaster University, Lancaster LA1 4YB, UK

**Abstract**

The dependence on measurement frequency and temperature of the depletion voltage extracted in the standard way from the CV characteristics of heavily irradiated silicon detectors is studied, parameterised and fitted. A similar pattern of behaviour is observed for a wide range of analysed detectors. A formula is derived which allows correction of the depletion voltage from one frequency-temperature point to another.

*PACS:* 07.77-n; 85.30.-z

Keywords: Irradiated silicon detectors; Depletion voltage; Frequency dependence; Temperature dependence

* Corresponding author. Tel:+44 1524 594627; fax: +44 1524 844037; E-mail address: a.chilingarov@lancaster.ac.uk

## 1. Introduction

Analysis of the CV characteristics is a standard method of measuring the depletion voltage ($U_d$) in semiconductor detectors. The principle of the method is simple: when the detector becomes fully depleted its capacitance should reach a minimal value, which does not depend on the bias voltage. To find $U_d$ a coordinate representation for the CV data is usually chosen, which produces an almost linear *x*-*y* dependence just below the depletion voltage. Typical examples of such representations are: log(C)-log(V), 1/C-$(V)^{1/2}$, 1/$C^2$-V. The sections of the CV curve below and above the assumed depletion voltage are fitted with straight lines and the *x*-coordinate of the crossing point of these lines is assumed to be the depletion voltage.

However, as noticed some time ago, the depletion voltage extracted in this way for Si detectors after heavy irradiation depends on the AC frequency [1] and on the temperature [1,2] at which the CV measurements are made. The temperature dependence can reflect a real change of $U_d$ with temperature. But the $U_d$ dependence on the AC frequency is clearly a systematic effect related to the measurement method itself because the depletion voltage is by definition a purely static parameter related to the electric field and/or space charge distribution inside the detector. Therefore $U_d$ should not depend on the frequency of the probing AC signal, which has an amplitude much smaller than the applied DC bias voltage.

The effects noticed in [1] were confirmed in a later work [3]. No coherent theoretical explanation of these experimental observations has emerged so far. In this situation there is a need for at least an empirical relation between the $U_d$ values measured at different frequencies and temperatures to allow for proper comparison between the $U_d$ measurements made under different conditions. The precision of the results and the frequency-temperature range used in the previous studies did not allow extraction of such a relation with reasonable

accuracy. The aim of the present work, performed as a part of the CERN RD48 (ROSE) Collaboration Project [4], is to address this need.

## 2. Experimental set-up

The measurements were performed with PIN diodes mounted on small PCB boards allowing contacts to be made to the diode back side, guard ring and the central part of the diode. An LCR meter HP 4284A with frequency range 20Hz-1MHz was used for the impedance measurements. The diodes were biased with a Keithley 2410 source-meter whose output voltage and current were read with an accuracy of $\pm$0.01V and $\pm$0.001$\mu$A, respectively. The whole system was controlled through a PC using an IEEE-488 interface. The online and offline programs were written with the LabVIEW software.

The circuitry chosen for the biasing of the diode and the C-V measurements is shown in Fig.1. Letters L and H denote the low and high sides of the 4-terminal input of the LCR meter. The Device Under Test (DUT) was installed in a copper DUT box cooled by a Peltier device. When at temperatures near and below 0°C the box was continuously flushed with dry nitrogen to avoid moisture build up. The other side of the Peltier element was cooled by mains water. This set-up permitted temperatures as low as -25°C to be achieved. The DUT box and its associated circuit elements were housed inside a metal box connected to ground.

Two decoupling capacitors $C_L$ and $C_H$ protect the LCR meter inputs from the DC voltages present in the circuitry. To minimise the effect of the circuitry on the impedance measurements, the values of the products $R_L C_L$ and $R_H C_H$ should be made as large as possible. The maximum values of $R_L$ and $R_H$ are limited by the maximum tolerable voltage drop across them due to the diode dark current. The maximum values of $C_L$ and $C_H$ are limited by their physical size and their corresponding voltage rating. A simple filter consisting of resistor $R_F$ and capacitor $C_F$ inside a grounded box reduces the noise from the source-meter.

The parameters of the circuit elements are listed below.

| Element | Value | Voltage rating |
|---|---|---|
| $C_L$ | 0.1μF | 1000V |
| $C_H$ | 10μF | 63V |
| $C_F$ | 1μF | 400V |
| $R_L$ | 226.1kΩ | |
| $R_H$ | 10.0kΩ | |
| $R_G$ | 9.9kΩ | |
| $R_F$ | 103.1kΩ | |

The total current through the DUT was measured by the source-meter. The ammeter on the ground side measured the current through the guard ring of the diode. The current through the diode centre was calculated as the difference $I_{cent} = I_{tot} - I_{gr}$. This was preferred to a direct measurement of the central current to minimise the interference on the LCR meter by the ammeter.

The actual values of the real and imaginary parts of the DUT impedance were calculated from the measured ones taking into account the effects of all the elements in the external circuitry. This calculation was done by the offline correction program, which also produced values of the different parameters describing the measured complex impedance e.g. parallel and serial capacitances and resistances, dissipation factor etc.

Open corrections were made with an empty PCB board to nullify the stray impedance of the set-up. The reconstruction of the impedance was checked with a standard 10pF capacitor mounted on the PCB board instead of a diode. At frequencies below 100Hz the reconstructed values of the test capacitor were found to be different by a few picofarads from its actual value measured at higher frequencies. Impedance offsets were calculated for the four frequencies: 20.5, 30.5, 63.5 and 97Hz and incorporated into the correction program. For any other

frequency below 100Hz the offsets were calculated by linear interpolation between the above four frequencies. For frequencies above 100Hz no offset corrections were needed.

Further verification of the system operation was made using the CV measurements taken with the non-irradiated diode R43. This is an *n*-type diode with overall dimensions of 7mm x 7mm x 314μm and a sensitive region of 5mm x 5mm surrounded by a guard ring. The measurements were taken at room temperature and at -24°C in either parallel $C_p$-$R_p$ or serial $C_s$-$R_s$ mode. For the non-irradiated diode the values of $C_p$ and $C_s$ are practically indistinguishable. Most of the results shown below are for parallel capacitance $C_p$.

In all our CV measurements the voltage was ramped downwards. For the diode R43 the range was from 150 volts to 3 volts with a 10% voltage step giving 42 voltage points. At each point 2 measurements were made allowing an estimation of the uncertainty of the result for each point. This was performed for frequencies 20.5Hz, 30.5Hz, 63.5Hz, 97Hz, 300Hz, 1kHz, 10kHz, 100kHz and 1MHz in a random order to suppress systematic errors in the frequency dependence. Fig.2 shows four measurements taken in the $C_p$ mode at the extreme ends of the frequency and temperature ranges. No significant difference can be seen between the CV curves in this plot above $U_{bias}$=10V, i.e. in the range used for the depletion voltage measurements. The values of the depletion voltage, $U_d$, and the depletion capacitance, $C_d$, were calculated from the cross-over point of the two straight lines in the log-log plot just below and above the beginning of the plateau in the capacitance values.

Figs.3 and 4 show $C_d$ and $U_d$, respectively, plotted against frequency at two temperatures for the $C_p$ and $C_s$ modes. As can be seen neither parameter is significantly dependent on frequency or temperature. The errors in $U_d$ reflect the uncertainty in the choice of the range for the straight line fits. The $C_d$ values are systematically higher than the value of 8.4pF calculated from the diode geometry. This is probably due to the effective sensitive area of the diode being slightly

larger than the nominal 25mm$^2$. The spread of the $C_d$ values at low frequencies shows the degree of reproducibility of the results for different measurements. The systematic variation of the $C_d$ values with frequency reflects the accuracy of calibration including all corrections.

The long-term stability of the system was checked over a period of 5 weeks with the non-irradiated diode R43 at room temperature for the three lowest frequencies i.e. 20.5Hz, 30.5Hz and 63.5Hz. No significant variations were observed. The results are summarised in Table 1.

**3. Studies of irradiated diodes.**

The diodes used for the study of the irradiated Si detector properties were produced by SINTEF[1]. Two of them: S54 and S62 were made from standard material. The other two R90, R98 were made from oxygenated Si produced by Polovodice within the RD48 program [4]. The diodes have a sensitive area 5x5 mm$^2$, surrounded by a guard ring, and a thickness of ~300μm. They were irradiated at room temperature and without bias at ISIS (RAL) by neutrons with energy of ~1MeV. The fluence was corrected to 1MeV neutron equivalent by multiplication by the hardness factor of 1.1 [5]. The fluence values and other characteristics of the detectors before and after irradiation are presented in Table 2.

Before irradiation all diodes had *n*-type conductivity i.e. positive space charge. After irradiation they all underwent the so-called "type-inversion", which should be more appropriately called "space charge sign inversion" since the properties of irradiated Si are very different from those of normal *p*-type material. After irradiation the diodes were kept at room temperature to allow beneficial annealing to take place. Their depletion voltage (monitored by the CV measurements at 10 kHz and 0$^o$C) decreased during several days and then

stabilised. After this the diodes were kept at subzero temperature to avoid reverse annealing.

The CV measurements were always made with the bias voltage decreasing from the maximum value (at least ~200V above the estimated depletion voltage) to the minimum one which was chosen to be 3V. It was noticed that ramping the bias voltage down gives more reproducible CV data than ramping it up. The amplitude of the AC signal was 1V. The depletion voltage was extracted from the two straight-line fits to the data in the log(C)-log(V) plot. An example is shown in Fig.5 for the diode S62 at 0°C and 3kHz. The solid lines are drawn through the points included in the fits; the dashed lines are the fit extrapolations. The *x*-coordinate of the crossing point gives the depletion voltage value $U_d$. The estimated uncertainty due to the choice of the fit ranges was taken as the error in $U_d$.

For frequencies $\geq$1kHz the depletion voltages obtained from the series and parallel mode measurements usually didn't differ within the errors. For lower frequencies the $U_d$ extracted from the $C_s$ data were systematically higher than those from the $C_p$ data. The reason for this is discussed in Section 7b. As an example a comparison between the $U_d$ values obtained in the two modes for the diode S62 at 0°C is presented in Fig.6. Clearly the value of $U_d$ extracted from the parallel mode is less sensitive to the measurement frequency. Therefore throughout the rest of the paper we use only the $C_p$ data.

It is well known that the CV characteristics of irradiated Si detectors become flatter with increasing frequency or with decreasing temperature. In our paper [6] we have shown that a simple scaling relates the frequency and temperature dependence of the CV curve shape. In the present study we restricted our analysis to the cases where the $C_pV$ characteristic is not too flat: i.e. the maximum $C_p$ value observed in the whole bias voltage range was higher by at least 15% than the plateau value achieved at high bias voltages. This criterion

[1] SINTEF Electronics and Cybernetics, P.O. Box 124, Blindern, N-0314 Oslo, Norway.

imposed an upper limit on the frequency used at each temperature. The lower frequency limit, 20Hz, was set by the LCR meter range.

As can be seen from Fig.6 the depletion voltage changes approximately linearly with the logarithm of the measurement frequency *f*. Therefore the following parameterisation was chosen for the $U_d$ dependence on *f*:

$$U_d = U_0 + dU * \log_{10}(f/1kHz) . \quad (1)$$

Here the parameter dU is the change in the depletion voltage when the frequency changes by a factor of 10 and parameter $U_0$ is the depletion voltage value at the reference frequency. The latter was chosen to be 1 kHz, which is approximately in the middle of the frequency range used in this study. The ratio of these two parameters was named the relative slope $\delta = dU/U_0$.

a) Measurements with one diode at 4 temperatures

The diode S62 was studied at 4 temperatures: -24°C, -12°C, -0.5°C and +12°C. In all cases the parameterisation (1) fitted well the dependence of the depletion voltage on frequency. The optimal values of the slope dU with the fit errors are presented in Fig.7 as a function of temperature. The decrease of the error with temperature is mostly due to the increase of the corresponding frequency range with temperature (see Fig.8). The maximum frequency is limited by the CV flatness criterion discussed in Section 3. As can be seen from Fig.7 no temperature dependence was observed for the parameter dU within the errors. Its average value is (–15.11± 0.43) V. To increase the accuracy of the parameter $U_0$ the fits were then repeated with dU fixed at its average value. The results shown in Fig.8 demonstrate both a good fit quality and the absence of systematic deviations of the data points from the parameterisation.

The optimal values for the parameter $U_0$ as a function of temperature are presented in Fig.9. The three low temperature values agree within the errors, while the value at +12°C is higher by ~3%. The relative spread in $U_0$ ~1.5% is considerably smaller than the spread of the dU values shown in Fig.7 which is

6.7%. The average relative slope can be calculated as the ratio of the average slope dU=–15.11V to the average $U_0$=162.3V obtained from the data in Fig.9 giving $<\delta>=-0.093\pm 0.006$. The error here is the 6.7% spread in the parameter dU and thus includes the possible deviation from the assumption of a temperature independent slope.

b) Measurements with 4 diodes at the same temperature

Another three irradiated diodes: S54, R90 and R98 were measured at one temperature only: -0.5°C. The depletion voltage values as a function of frequency for all 4 diodes at this temperature are shown in Fig.10 together with the fits by equation (1). The errors are usually of the order of the symbol size and therefore are not shown on the plot. The fit quality is generally reasonable though the values of the $\chi^2/N_{df}$ shown in Table 2 are always higher than 1. Therefore the errors for parameters dU and $U_0$ found from the fits were increased by a factor of $(\chi^2/N_{df})^{0.5}$.

As is clearly visible in Fig.10, the reference depletion voltage grows and the slope of the lines becomes steeper with the increase of the irradiation fluence. However as can be seen at Fig.11 the relative slope $\delta$ is practically the same for all diodes with a weighted average $<\delta>=-0.103\pm 0.008$. In this expression the actual spread of $\delta$ for the individual diodes from its average value is taken as the error. Thus it includes the possible deviation from the assumption that $\delta$ is independent of the irradiation fluence and the material of the diodes.

**4. Reanalysis of our previous data.**

As mentioned in the Introduction we first demonstrated the dependence of the depletion voltage on the measurement frequency for irradiated Si diodes in our publication [1]. In that work we also investigated the dependence of $U_d$ on temperature, which at that time had already been announced in the literature [2].

To simplify the comparison between our present and previous results we reanalyse in this section our data published in Ref.[1] using the parameterisation (1).

Most of the measurements described in Ref. [1] were made with the diode M41, which has a geometry similar to that described above. It was produced by Micron Semiconductor Ltd. (Lancing, UK) from standard *n*-type Si and was irradiated by neutrons at ISIS (RAL) with 1MeV equivalent fluence $1.1 \cdot 10^{14}$ n/cm$^2$. The irradiation and annealing conditions were identical to those described in Section 3.

The $C_pV$ data were measured at frequencies 1,10,20 and100 kHz in the temperature range –16$^o$C - +32$^o$C. Using the same CV flatness criterion as above we have limited the higher frequency for each temperature. As a result the measurements at subzero temperatures were left with less than three valid frequency values and therefore were not included in the $U_d$ versus frequency analysis. The fits by equation (1) to the remaining 5 data sets are presented in Fig.12. These fits were performed with equal weights ascribed to the data points and the errors of the fitted parameters were calculated from the spread of the points relative to the fit line. The resulting values of the relative slope $\delta$ as a function of temperature are shown in Fig.13. Again no temperature dependence is observed within the errors. The average $\delta$ value is $<\delta>=-0.126 \pm 0.010$. As above the error here is the spread of the data points rather than the standard error for the average value.

The optimal values for the reference depletion voltage $U_0$ as a function of temperature are shown in Fig.14. The points at –16$^o$C and –8$^o$C are the $U_d$ values measured at 1 kHz, hence their larger errors. As with the data in Fig.9 the points at low temperatures are consistent with each other, while the values at higher temperature clearly grow with temperature.

## 5. Analysis of the data from the other sources

The data published in Ref. [3] for a microstrip detector irradiated by 24GeV protons up to $3 \cdot 10^{14}$ p/cm$^2$ and measured before beneficial annealing were also analysed with our parameterisation. The $U_d$ data versus frequency for 3 temperatures from Fig.4 of Ref. [3] were fitted using the function (1). The results are shown in Fig.15. There is a hint of saturation for the $U_d$ values below 100Hz. However the spread of the points in general is rather large and in addition the measurements at low frequencies are difficult which implies larger errors compared to those at higher frequencies.

The values of the relative slope $\delta = dU/U_0$ as a function of temperature are presented in Fig.16 with the errors calculated from the spread of the points around the straight lines in Fig.15. The spread of the $\delta$ values is much smaller than their errors, which indicates that the nature of the errors in $\delta$ is more systematic than statistical. Therefore the error for the average $\delta$ value was calculated as an average error of the points in Fig.16 to reflect the fact that the systematic errors with the same origin are not decreased by averaging. The result is $<\delta> = -0.148 \pm 0.032$.

The data for the depletion voltage dependence on temperature are given in Fig.3 of Ref. [3] for 3 frequencies: 0.2, 0.5 and 1 kHz. To increase the accuracy the data for each temperature point were averaged. The results are presented in Fig.17. In agreement with the results discussed above (Figs. 9 and 14) no dependence is visible within the temperature range $-20^o$ to $0^o$C. The errors here represent a 5.1% spread of the points relative to their average value.

In our paper [7] we described the measurements with two diodes #79 and #81 produced from standard *n*-type Si, irradiated by neutrons with 1MeV equivalent fluences of 0.6 and $2.4 \cdot 10^{14}$ n/cm$^2$ and annealed to a minimum depletion voltage

(see Ref.[7] for further details). Our collaborators at Hamburg University have complemented the standard CV data at 10 kHz, used for the $U_d$ measurements in Ref.[7], by the CV characteristics for 0.12, 1.0 and 100 kHz. All measurements were made at +22$^o$C. Using the approach described in Section 3 we have extracted the depletion voltage from the CV data measured in Hamburg. The depletion voltage as a function of frequency for these diodes is presented in Fig.18 together with the fit by equation (1). The fit quality is very good. The values for the relative slope $\delta$ are: -0.183 $\pm$ 0.051 and -0.140 $\pm$ 0.015 for diodes #79 and #81, respectively. They agree within their errors and their weighted average is: $<\delta>$= -0.143 $\pm$ 0.014.

## 6. Comparison of the available data

a) Relative slope $\delta$

A summary of the results for the relative slope $\delta$ obtained as described above from different sources is presented in Table 3. The 24 GeV proton fluence from the Ref.[3] was converted to 1MeV neutron equivalent fluence using hardness factor 0.62 [8].

There is an impression that the absolute value of $\delta$ increases with the average temperature at which the measurements were performed. However this is not observed when the slope is measured within a wide temperature range in the same experiment (see Figs.7 and 13). The $\delta$ values from the last column of Table 3 do not quite agree within their errors. The $\chi^2/N_{df}$ relative to their weighted average is 4.4. With the error multiplied by the square root of the latter value the weighted average $<\delta>_w$=-0.106$\pm$.009. When all $\delta$ values are simply averaged with equal weight the result is $<\delta>_s$=-0.123$\pm$.024, where the error is the r.m.s. of the individual values. It is debatable which averaging method should be preferred. Therefore as a global estimate for $\delta$ we use the average of the two above numbers as a central value and the spread of the points as an error. The

result: $<\delta>_g$=-0.114±.024 covers within one quoted error three of five $\delta$ values from Table 3, and all of them lie within two errors. Within its uncertainty this result is valid for the whole investigated range in temperature: –24°C to +32°C and fluence (0.4-2.4)·$10^{14}$ n/$cm^2$, and for all 8 detectors used in this study.

b) Reference value as a function of temperature

As can be seen from Figs. 9 and 14 the reference value $U_0$ is practically independent of temperature for the measurements at or below 0°C. To simplify the comparison of the temperature dependence for different detectors we normalised the $U_0$ values by their weighted average, $U_0$(lt), at low temperatures (below 1°C). Fig.19 shows the results for detectors S62 and M41 from Figs.9 and 14, respectively, normalised in this way. The data for the two detectors agree well and were fitted together by the following expression:

$$U_0/U_0(lt) = 1 + A \exp[-(E_a/k)(1/T - 1/T_0)] \qquad (2)$$

with $T_0$=273.15K (0°C). This equation assumes that at low temperatures the space charge density and hence the depletion voltage remain constant. The parameter $U_0$(lt) is the asymptotic value of $U_d$ at low temperatures. At higher temperatures an additional space charge develops with density growing in the usual exponential way, which results in a corresponding growth of the depletion voltage. Parameter A is the deviation of the depletion voltage at 0°C from its asymptotic value. The result of the fit by equation (2) is shown by the curve in Fig.19.

The fit quality is good: $\chi^2/N_{df}$=1.05. The values of the parameters obtained from the fit are: A=0.0086±0.0016 and $E_a$= 0.635±0.050 eV. The value of A is small enough to justify the temperature range used for the normalisation of the data from Figs.9 and 14. The activation energy $E_a$ has a value close to half the band gap for Si, which is typical for the temperature dependencies in this material. At a standard temperature of 300K or 27°C (which is probably the highest temperature suitable for CV measurements with heavily irradiated silicon

detectors) the deviation of the depletion voltage from its asymptotic value reaches 10%.

Three more sets of experimental data are available in the literature for the discussed temperature range. One of them from Ref.[3] was analysed above and is presented in Fig.17. The second is from Ref. [2] measured for several irradiated diodes at temperatures from $0^{o}$ to $+50^{o}$C. The third was extracted from the CV characteristics published in Ref.[9] and the values of $U_d$ were provided by one of the authors of Ref.[9] (M.McPherson). The latter measurements were performed in the temperature range $-24^{o}$ - $+70^{o}$C for a Si diode irradiated by fluence $0.3 \cdot 10^{14}$ n/cm$^2$. These 3 data sets, normalised in the same way as the data in Fig.19, are presented in Fig.20 together with the data and the fit curve from Fig.19. To remain not very far from the temperature range studied in this work we have limited the maximum temperature in this plot to $+45^{o}$C. One can see that the other published data on the temperature dependence of the depletion voltage agree well with our results, which however have a much better accuracy.

In contrast to the frequency dependence, which is a systematic effect of the measurement method (see Introduction), the dependence of the depletion voltage on temperature can reflect a real change of the voltage at which the whole detector volume becomes depleted of free carriers. At cryogenic temperatures such effects were clearly demonstrated by the RD39 Collaboration in measurements of the detector response to ionising particles [10]. In the present study it is impossible to separate the real temperature dependence of the $U_d$ from the systematic effects related to the CV method itself. But in any case the observed dependence, which is found to be valid for a wide range of Si detectors, can be used for a proper comparison of the $U_d$ values obtained by the CV method at different temperatures.

## 7. Discussion

a) Visualisation of the $U_d$ shift with frequency

It is well known that the CV characteristics of irradiated diodes become flatter and change their overall shape when the frequency increases for a fixed temperature. Therefore, if several CV curves corresponding to very different frequencies are put in one plot, it is difficult to see clearly the shift of the "kink" position in these data. To make the $C_pV$ curves for the frequencies of 30Hz, 3kHz and 86kHz more easily comparable visually in the vicinity of the depletion voltage, the data measured for the diode S62 at +12$^o$C were transformed in the following way. The capacitance values at all points were normalised by the plateau value $C_{dp}$ defined as the average capacitance in the $U_{bias}$ interval 220-320 V. The normalised values were then raised to a power $\alpha$ defined so that $(C/C_{dp})^{\alpha}=2$ at $U_{bias}=80$V which is about half of the reference depletion voltage $U_0$ for this diode. This corresponds to a shift of the capacitance data in the logC-logV plot to a common plateau level with a subsequent scaling from this level of the vertical coordinate for each frequency in such a way that all curves acquire the same scale in the bias voltage range between $U_d/2$ and $U_d$. Obviously this procedure only shifts and turns the straight lines, selected in the original logC-LogV plot (see Fig.5), but it does not make them curved. The values of $C_{dp}$ and $\alpha$ used for this transformation are shown in Table 4.

The results are presented in Fig.21. One can see that the horizontal position of the crossing point for the two straight lines drawn in the usual way clearly shifts downward when the frequency increases. In other words a sharp change in the capacitance dependence on bias voltage from a relatively steep to a relatively slow variation happens at lower voltages for higher frequencies. This behaviour

should also appear in other possible data representations: e.g. 1/C vs. $V^{1/2}$ or $1/C^2$ vs. V. Therefore the dependence of the depletion voltage on frequency should be qualitatively the same for any choice of the CV representation, though some quantitative differences may appear. This was confirmed by an independent analysis of our CV data performed by the ATLAS Dortmund group [11]. In the absence of a theoretical model for the CV curve of a heavily irradiated silicon detector we prefer the logC-logV coordinates as the most general presentation of the data since it gives a linear dependence for any power of the bias voltage.

b) The difference in $U_d$ extracted from the $C_p$ and $C_s$ data

In Section 3 it was mentioned that for low frequencies the depletion voltage values extracted from the CV data measured in the series mode $C_s$-$R_s$ are systematically higher than those for the parallel mode $C_p$-$R_p$. The reason for this can be understood from Fig.22. It shows $C_p$, $C_s$ and the dissipation factor $D=1/\omega C_p R_p$ as a function of bias voltage for the measurements performed with diode S62 at 30Hz and $+12^oC$. The dissipation factor in this figure is presented as a percentage to have the same scale as for the capacitances.

One can see that for $U_{bias}$ above 200V the $C_p$ remains constant indicating full depletion of the detector. However the parallel resistance $R_p$ and hence dissipation factor continues to change with $U_{bias}$. From the relation $C_s=C_p\cdot(1+D^2)$ it is clear that if $D^2$ is not small compared to 1 a variation in D leads to a variation in $C_s$ even for a stable value of $C_p$. As a result the "kink" position in the $C_s$-V data is shifted upward compared to that in the $C_p$-V data. Since the parallel equivalent circuit is a more appropriate description of the fully depleted detector, the depletion voltage for the $C_s$ data is artificially boosted due to: a) the large dissipation, and b) the variation of the detector bulk conductivity with voltage above full depletion. For high frequencies the dissipation factor D becomes small which leads to closer values of $C_s$ and $C_p$ and as a result to closer $U_d$ values.

c) Possible reasons for the $U_d$ frequency dependence.

The fact, that the parallel resistance of the diode bulk continues to evolve significantly with the bias voltage above full depletion and stabilises at noticeably higher voltages than the parallel capacitance, gives a hint to the possible reasons for the dependence on frequency of the depletion voltage. The latter can be interpreted as the different threshold voltages required for the stabilization of the parallel capacitance $C_p$ at different frequencies. This may be due to the different behaviour with bias voltage of the irradiated silicon dielectric constant $\varepsilon$ (complex and frequency dependent in the general case) at different frequencies. The change of the resistance with voltage discussed above may also be due to the change in $\varepsilon$ via its imaginary part (the so-called AC losses). All this is quite feasible because the properties of the bulk in a reverse biased irradiated detector are related to the occupancy state of numerous deep level defects produced by the irradiation, which may change with bias voltage. Simultaneously this implies that the relations for $U_d$ measured at different frequencies and temperatures obtained above (equations 1 and 2) may not necessarily be true for detectors made from substantially modified material (e.g. strongly oxygenated) or measured at a different annealing stage (e.g. after reverse annealing).

d) Corrections for the dependence of $U_d$ on frequency and temperature

The results of this work are applicable first of all to detectors made of ordinary (or nearly ordinary) silicon irradiated by 1 MeV neutron equivalent fluence in the range $(0.5–2.5)\cdot10^{14}$ n/cm$^2$ and beneficially annealed. They concern the depletion voltage extracted in the standard way from the $\log(C_p)$-$\log(V)$ characteristics measured at temperatures between –25°C and +35°C at frequencies for which the C-V characteristics are not very flat (see Section 3). These limits however include many of commonly made measurements. The relations derived in this work allow a correct comparison of the results obtained

under different conditions. As an example, below is the expression (3) recommended for correction of the depletion voltage extracted from the $C_pV$ data measured at temperature $T$ and at frequency $f$ to a "standard" frequency-temperature point chosen at the conditions often used in practice: $f_s$=10kHz, $T_s$=293.15K (20°C).

$$U_d(10\,kHz, 20^o C) = U_d(f,T)\frac{1+Ae^{\frac{E_a}{0.345eV}}}{1+Ae^{\frac{E_a}{0.02354eV}\frac{T-273{,}15K}{T}}}\frac{1+d}{1+d\log_{10}(\frac{f}{1kHz})} \qquad (3)$$

The recommended values for the parameters in this formula with their errors are: $d$=-0.114±0.024; $A$=0.0086±0.0016; $E_a$=(0.635±0.050) $eV$. For example the correction coefficient from a measurement performed at –10°C with frequency 100Hz will be 0.84. It includes a 21% decrease due to the frequency correction and a 5% increase due to the temperature correction. For a typical 300V depletion voltage of an irradiated Si detector this correction will be ~50V.

## 8. Conclusion

The dependence of the depletion voltage for heavily irradiated silicon detectors, extracted from the CV characteristics, on measurement frequency and temperature was studied for a range of detectors. For all of them the depletion voltage is observed to decrease logarithmically with frequency and to be independent of temperature below 0°C but rising with temperature above this. A formula, which parameterises this behaviour (equation 3), was obtained from the fit to the data. This formula allows measurements made at frequency $f$ and temperature $T$ to be corrected to a standard point $f_s$-$T_s$. Such corrections can be quite significant for the temperature and frequency range used in recent studies.

The difference between the values of the depletion voltage obtained from the parallel and series measurements at low frequencies is shown to be due to the large dissipation factor for these frequencies and to the variation of the detector resistance with bias voltage above full depletion. A similar variation of the

dielectric constant for the depleted bulk is discussed as a possible reason for the frequency dependence of the depletion voltage.

**Acknowledgements**

The authors are grateful to Eckhart Fretwurst for the CV data for two of the investigated diodes, as well as to Petra Riedler and to Mike McPherson for the numerical values of their published results. They are also grateful to Lars Evensen (SINTEF) for providing the diodes for this and other radiation damage studies, and to Brian K. Jones for fruitful discussions.

**References**

[1] L.Beattie, A.Chilingarov, P.Ratoff, T.Sloan, "Dependence of the depletion voltage and capacitance on temperature and frequency in heavily irradiated silicon diodes", ROSE Technical Note 97/4, March 1997.
[2] J.A.J.Matthews et al., Nucl.Instr.and Meth. A 381 (1996) 338.
[3] D.Morgan, P.Riedler et al., Nucl.Instr.and Meth. A 426 (1999) 366.
[4] RD48/Rose Collaboration homepage http://rd48.web.cern.ch/RD48/.
[5] T.Angelescu, A.Vasilescu, Nucl.Instr.and Meth. A 374 (1996) 85.
[6] D.Campbell, A.Chilingarov, T.Sloan, Nucl.Instr.and Meth. A 466 (2001) 456.
[7] T.J.Brodbeck et al., Nucl.Instr.and Meth. A 455 (2000) 645.
[8] G.Lindstroem et al., Nucl.Instr.and Meth. A 466 (2001) 308.
[9] B.K.Jones, J.Santana, M.McPherson, Nucl.Instr.and Meth. A 395 (1997) 81.
[10] K.Borer et al., Nucl.Instr.and Meth. A 440 (2000) 5.
[11] A.Borowski, O.Krasel, "Evaluation of CV-Curves" Proc. of 1st Workshop on Quality Assurance Issues in Silicon Detectors, CERN, May 2001, CERN-Proceedings-2001-001, pp.437-443, Geneva, June 2001.

Table 1: Stability of the depletion voltage and the depletion capacitance of non-irradiated diode R43 at low frequencies over a period of 5 weeks.

| Frequency (Hz) | Mean $U_d$ (V) | $\sigma U_d$ (V) | Mean $C_d$ (pF) | $\sigma C_d$ (pF) |
|---|---|---|---|---|
| 20.5 | 36.70 | 0.54 | 9.58 | 0.29 |
| 30.5 | 36.89 | 0.38 | 9.59 | 0.13 |
| 63.5 | 36.96 | 0.18 | 9.31 | 0.07 |

Table 2. Characteristics of the detectors used in the present study.

| Detector Name | R43 | S54 | S62 | R90 | R98 |
|---|---|---|---|---|---|
| Thickness (μm) | 314 | 344 | 335 | 285 | 284 |
| Fluence ($10^{14}$1MeV n/cm$^2$) | 0 | 0.45 | 0.82 | 1.6 | 2.2 |
| $U_d$ before irradiation (V) | 37.4 | 40.1 | 26.3 | 90.4 | 87.7 |
| $U_d$ after irrad. and annealing (V) | N/A | 72.2 | 146.5 | 188.2 | 261.7 |
| $\chi^2/N_{df}$ for the $U_d$ vs f fit at 0$^o$C | N/A | 2.3 | 2.5 | 7.3 | 4.5 |

Table 3. Relative slope obtained in different experiments.

| Source | No of detectors | Temp.range ($^o$C) | Fluence range ($10^{14}$n/cm$^2$) | δ |
|---|---|---|---|---|
| This work | 1 | -24$^o$ - +12$^o$ | 0.8 | -0.093±.006 |
| This work | 4 | -0.5$^o$ | 0.4 – 2.2 | -0.103±.008 |
| Ref. [1] | 1 | 0$^o$ - +32$^o$ | 1.1 | -0.126±.010 |
| Ref. [3] | 1 | -10$^o$ - 0$^o$ | 1.9 | -0.148±.032 |
| This work | 2 | +22$^o$ | 0.6 – 2.4 | -0.143±.014 |

Table 4. Parameters $C_{dp}$ and $\alpha$ used for the normalisation of the data presented in Fig. 21.

| Frequency (kHz) | $C_{dp}$ (pF) | $\alpha$ |
|---|---|---|
| 0.03 | 8.13 | 0.6362 |
| 3 | 8.22 | 0.9411 |
| 86 | 7.91 | 5.847 |

## Figure Captions:

Fig.1. Circuit diagram for the CV measurements.

Fig.2. $C_pV$ measurements for the non-irradiated diode R43 at room temperature (RT) and -24°C at frequencies 20.5Hz and 1MHz.

Fig.3. Depletion capacitance for the non-irradiated diode R43 measured in the parallel ($C_p$) and serial ($C_s$) modes at room temperature (RT) and -24°C.

Fig.4. Depletion voltage for the non-irradiated diode R43 measured in the $C_p$ and $C_s$ modes at room temperature (RT) and -24°C.

Fig.5. Example of the depletion voltage extraction from the $C_pV$ characteristics. The data are for the diode S62 at $0^{o}$C and 3 kHz. The solid lines are drawn through the points included in the fits; the dashed lines are the fit extrapolations.

Fig.6. Depletion voltage extracted from the $C_pV$ and $C_sV$ curves for the diode S62 at 0°C.

Fig.7. Fitted values for the parameter dU of equation (1) as a function of temperature for the diode S62.

Fig.8. Depletion voltage as a function of frequency for the diode S62 measured at temperatures: -24°C and -12°C (a); -0.5°C and +12°C (b). The lines are the fits by equation (1) with the parameter dU fixed at –15.11V.

Fig.9. Parameter $U_0$ from the fits shown in Fig.8 as a function of temperature.

Fig.10. Depletion voltage as a function of frequency measured at -0.5°C for 4 diodes irradiated by different fluences. Also shown are the fits by equation (1) with both parameters free. The errors for the points are of about the symbol size.

Fig.11. The relative slope $dU/U_0$ as a function of fluence extracted from the fits presented in Fig.10.

Fig.12. Depletion voltage as a function of frequency for the diode M41 at five temperatures. The data from our previous publication [1] are fitted using equation (1).

Fig.13. Relative slope $dU/U_0$ for diode M41 as a function of temperature extracted from the fits shown in Fig.12.

Fig.14. Parameter $U_0$ as a function of temperature for the diode M41. See text for the details of its extraction and errors.

Fig.15. Data on the depletion voltage versus frequency at three temperatures from Ref. [3] fitted by the equation (1).

Fig.16. Relative slope $dU/U_0$ obtained in the fits at Fig.15 as a function of temperature.

Fig.17. Depletion voltage as a function of temperature from Ref.[3]. The data are the average for measurements at frequencies of 0.2, 0.5 and 1kHz. The errors represent a 5.1% spread of the points around their average value.

Fig.18. Depletion voltage as a function of frequency measured at $+22^oC$ for the diodes #79 (a) and #81 (b) used in Ref.[7] together with the fits by equation (1).

Fig.19. The data from Figs.9 and 14 normalised by their average values below $1^oC$. The line is the fit by equation (2).

Fig.20. Comparison of the data from Fig.19 (●) with the other published data: Ref.[3]-(◊), Ref.[2]-(o) and Ref.[9]-(∇). See text for further details.

Fig.21. $C_p$-V dependence for the diode S62 measured at $+12^oC$ for three frequencies. The data were normalised to the same plateau level and to the same value at $U_{bias}$=80V as described in the text and in Table 4.

Fig.22. Parallel capacitance $C_p$, serial capacitance $C_s$ and the dissipation factor D measured with diode S62 at $+12^oC$ and 30Hz.

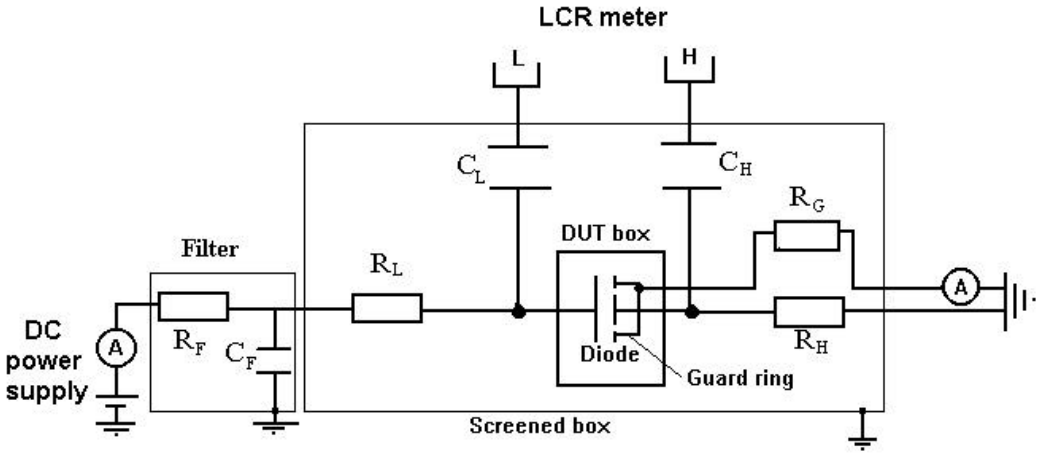
LCR meter
L
H
$C_L$
$C_H$
$R_G$
DUT box
Filter
$R_L$
A
DC
power
supply
A
$R_F$
$C_F$
Diode
Guard ring
$R_H$
Screened box

Fig.1

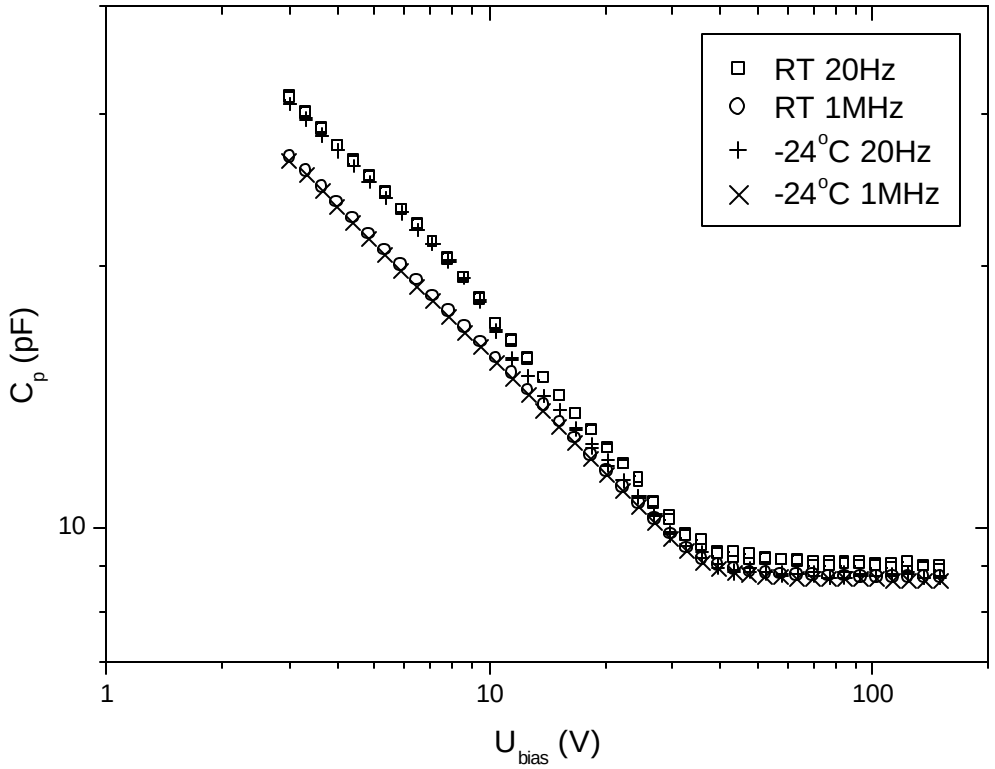


Fig.2

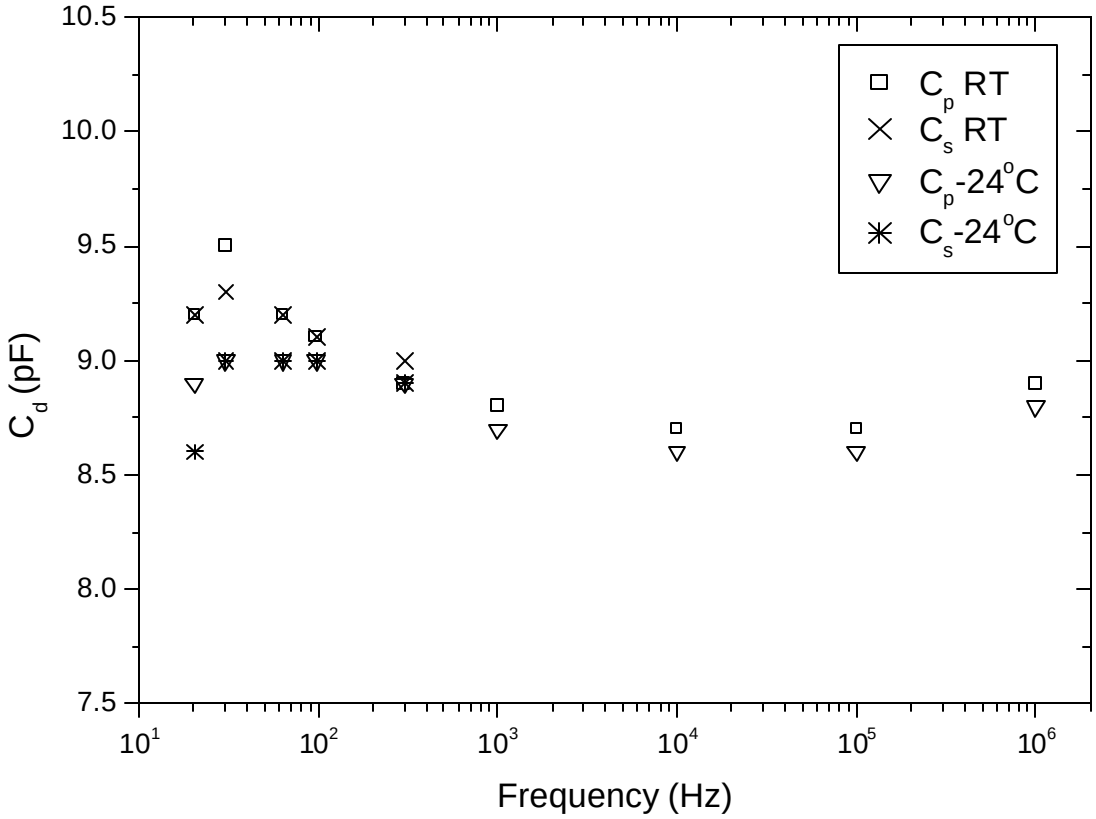
10.5
10.0
9.5
9.0
8.5
8.0
7.5
$C_d$ (pF)
$10^1$
$10^2$
$10^3$
$10^4$
$10^5$
$10^6$
Frequency (Hz)
$C_p$ RT
$C_s$ RT
$C_p$-24°C
$C_s$-24°C

Fig.3

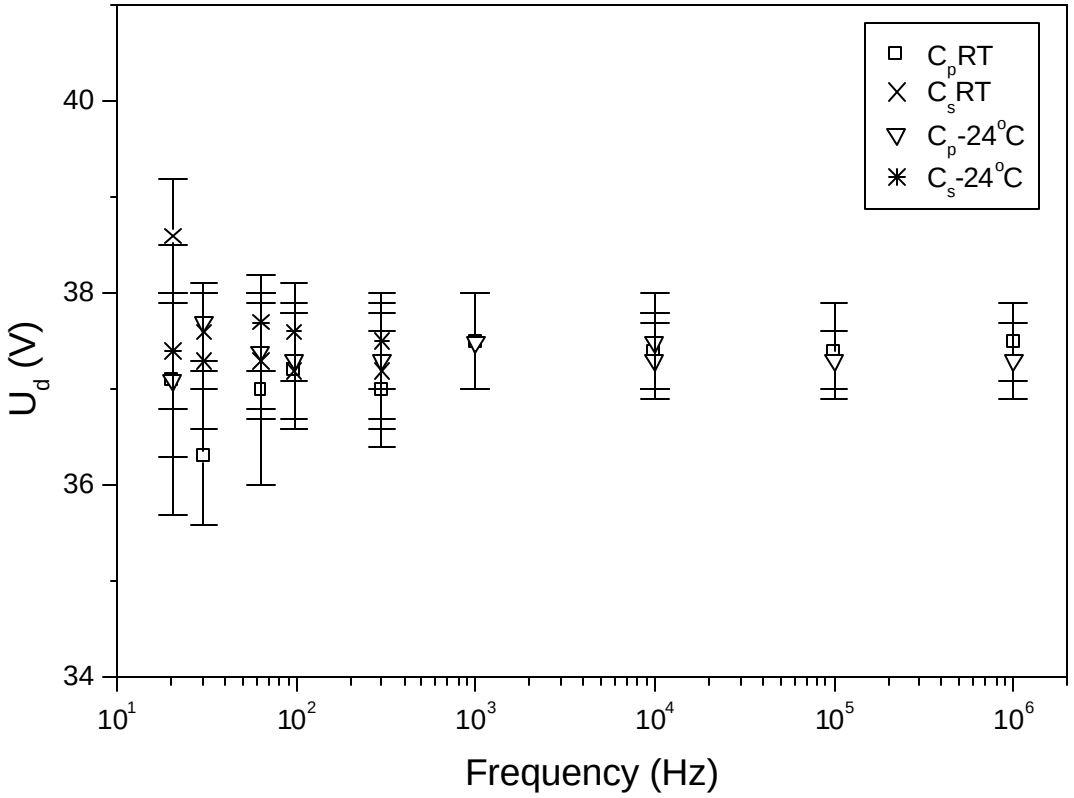
C_pRT
C_sRT
C_p-24°C
C_s-24°C
40
38
36
34
U_d (V)
10^1
10^2
10^3
10^4
10^5
10^6
Frequency (Hz)

Fig.4

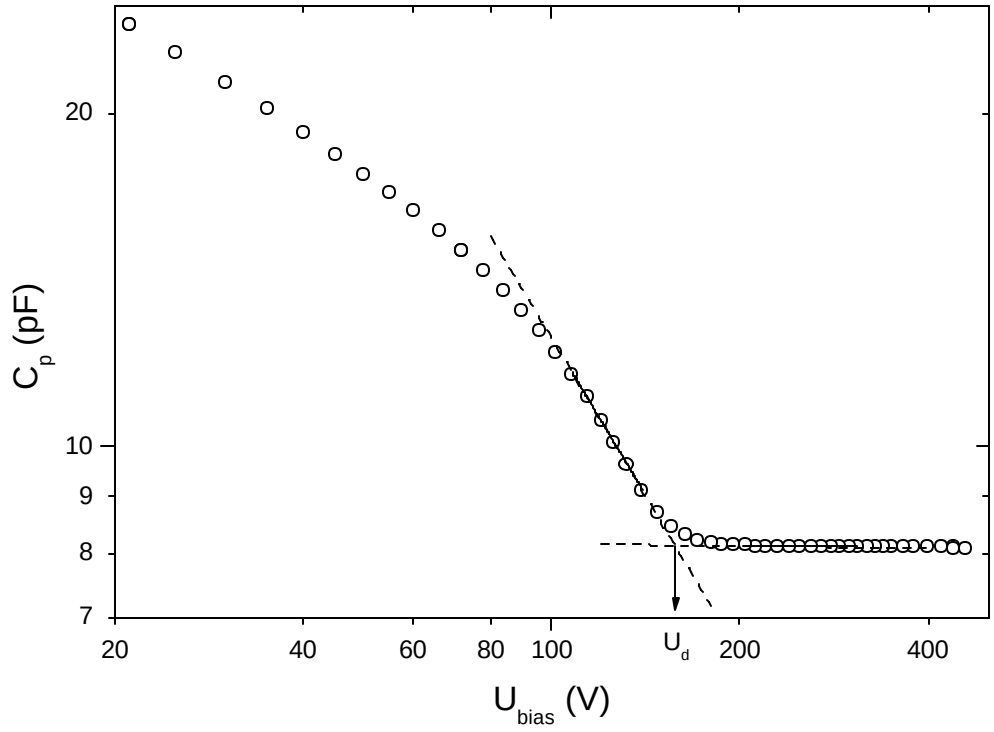


Fig.5

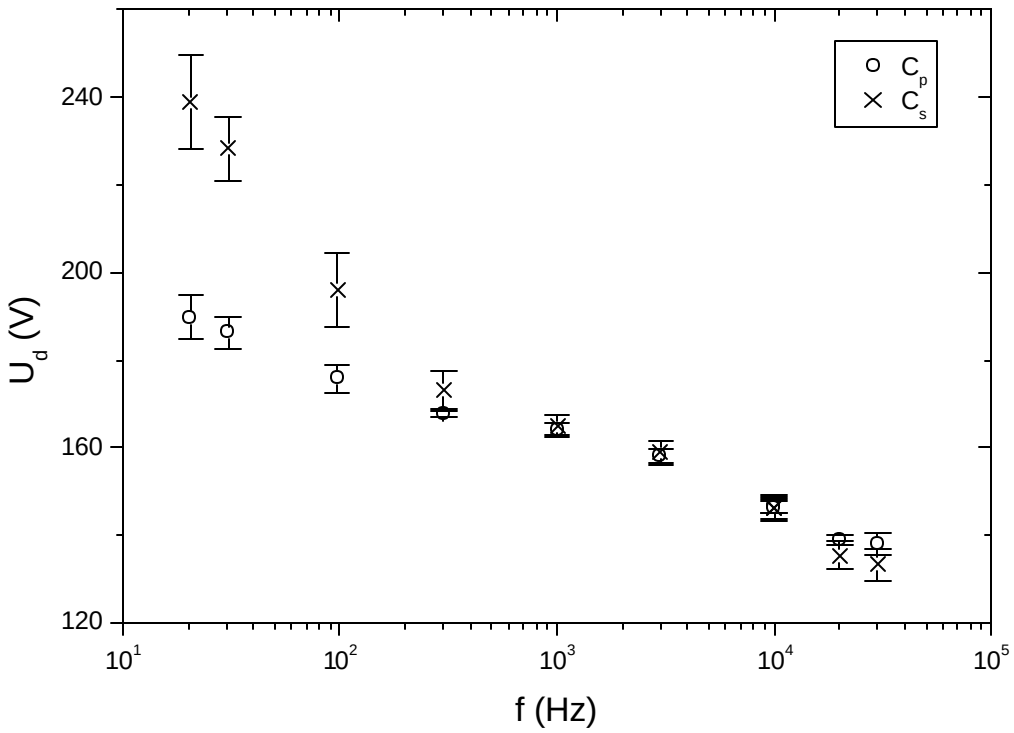


Fig.6

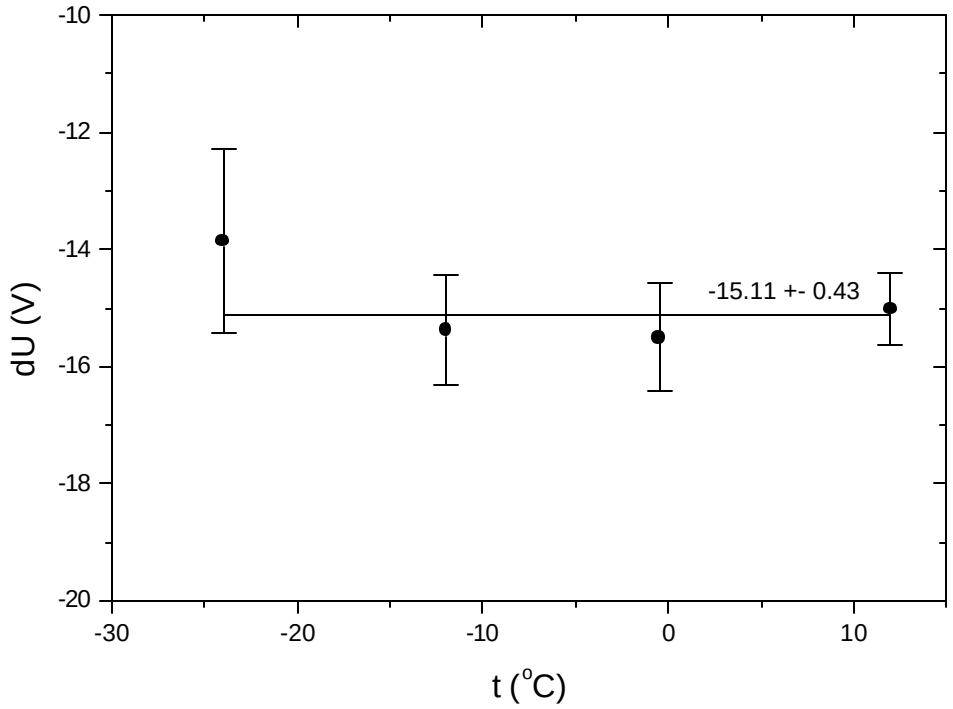


Fig.7

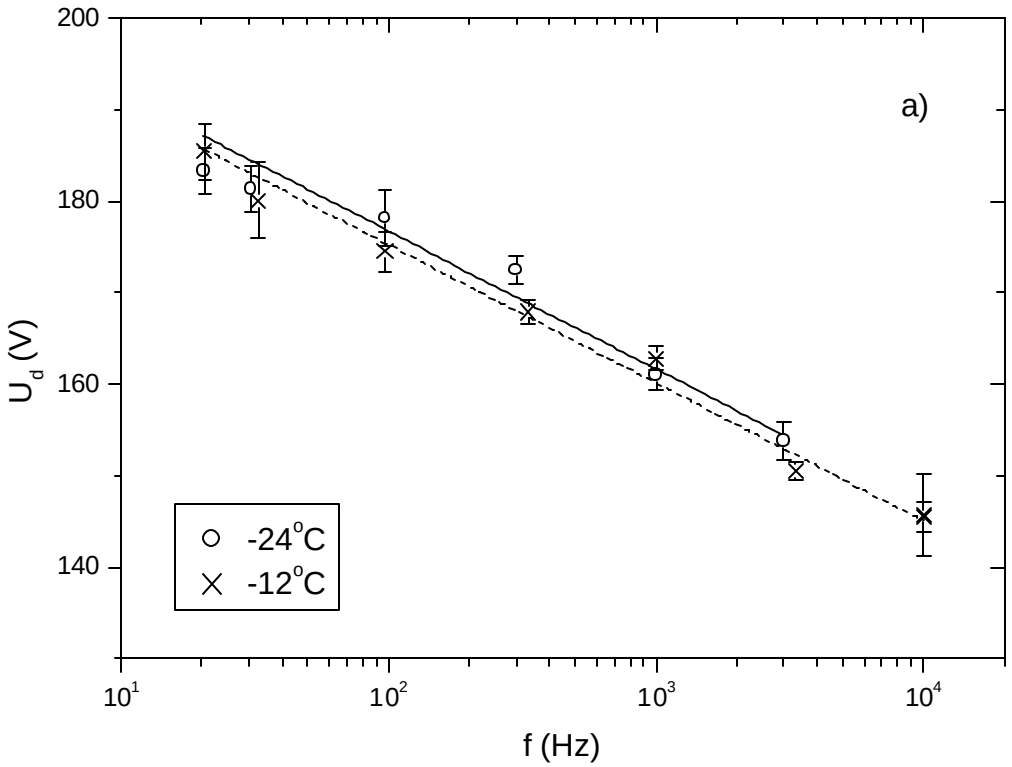


Fig.8a

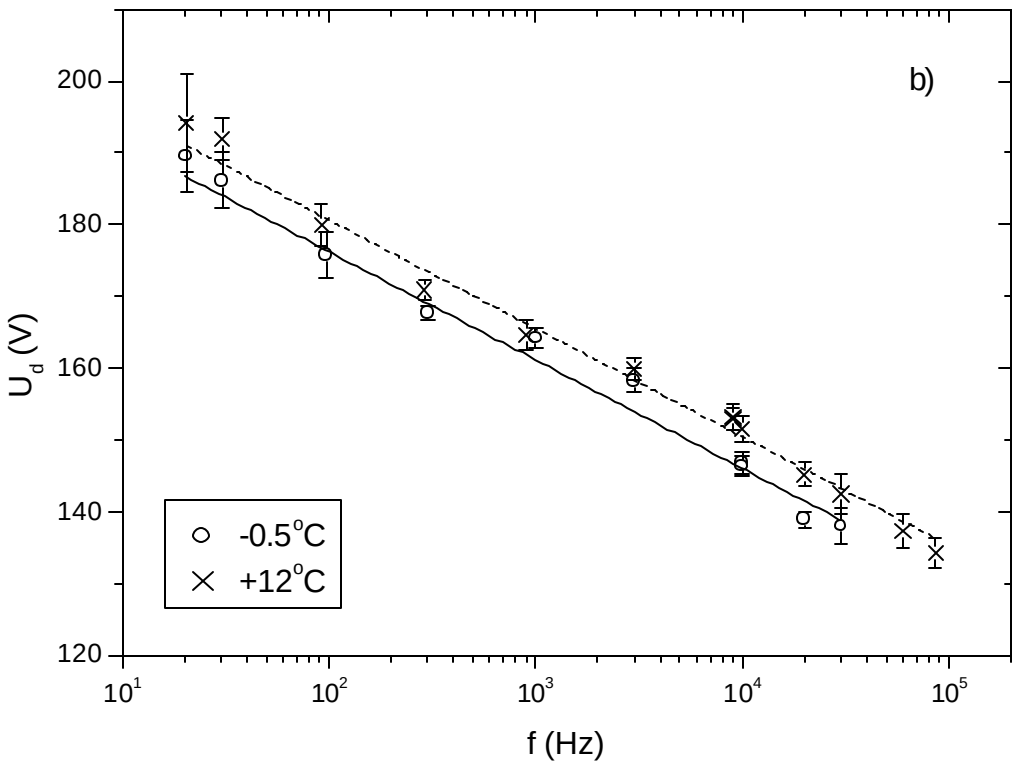


Fig.8b

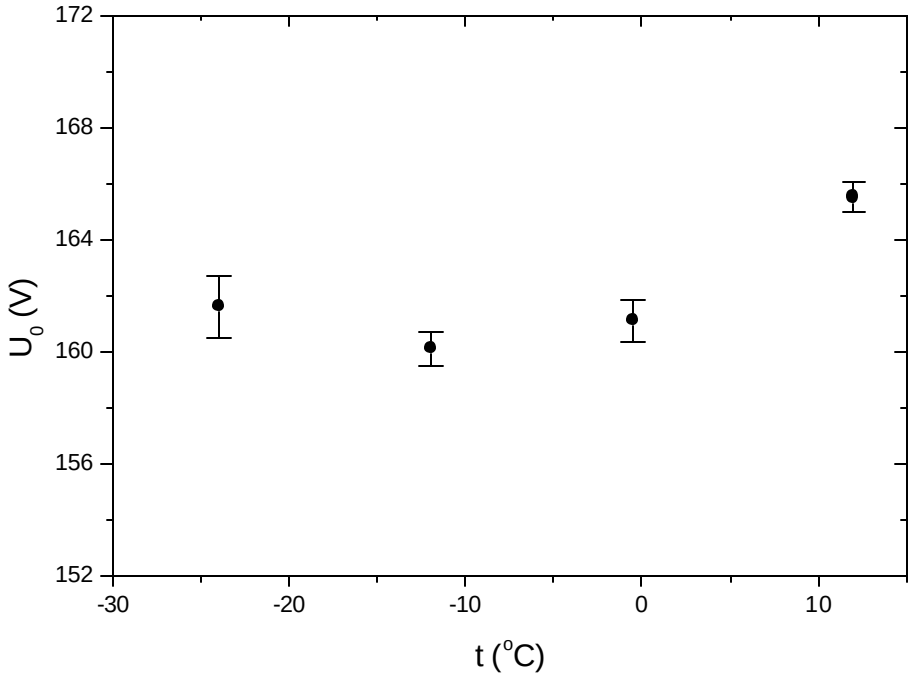


Fig.9

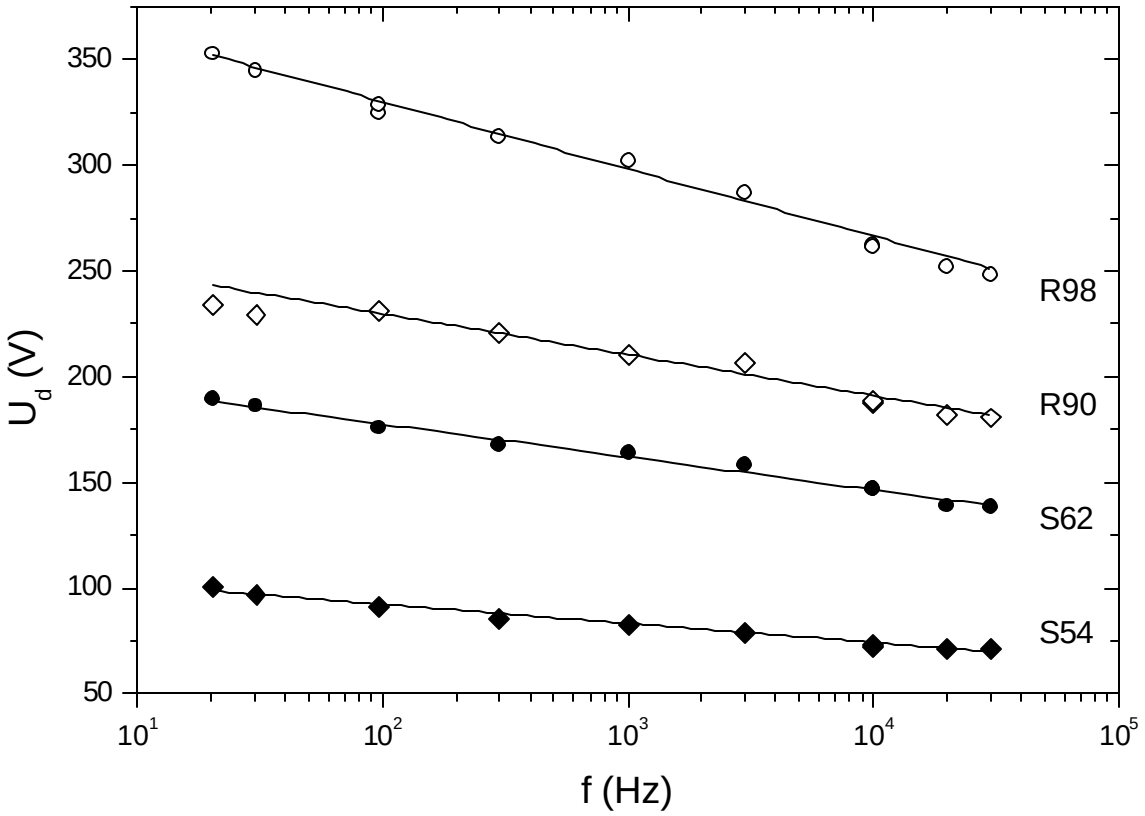
350
300
250
200
150
100
50
$U_d$ (V)
$10^1$
$10^2$
$10^3$
$10^4$
$10^5$
f (Hz)
R98
R90
S62
S54

Fig.10

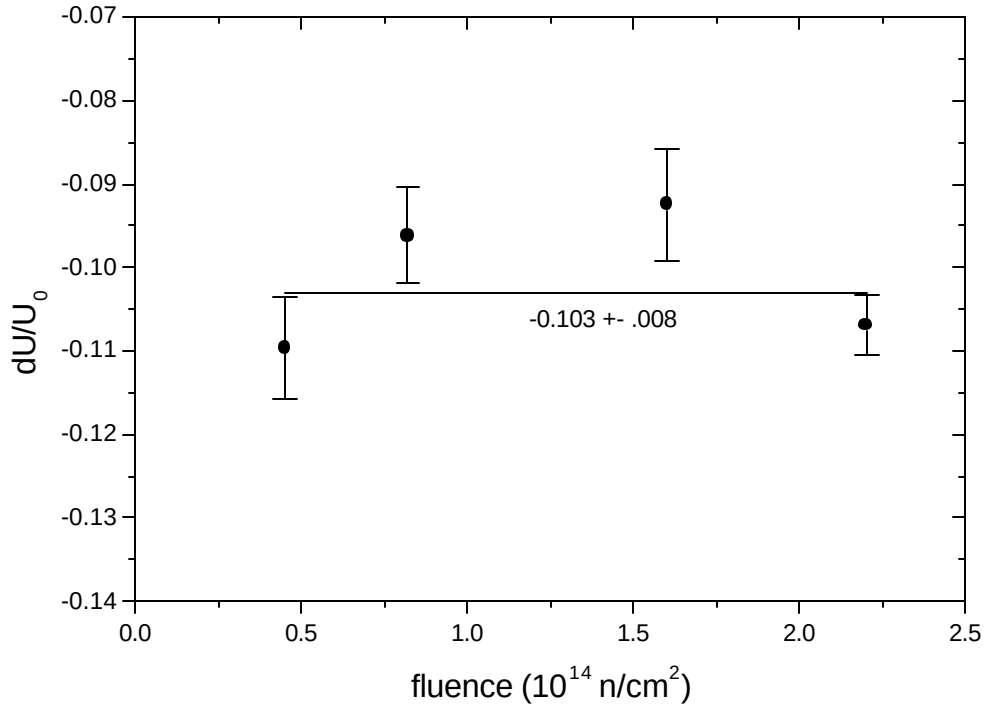
-0.07
-0.08
-0.09
-0.10
-0.11
-0.12
-0.13
-0.14
dU/U0
0.0
0.5
1.0
1.5
2.0
2.5
-0.103 +- .008
fluence (10^14 n/cm^2)

Fig.11

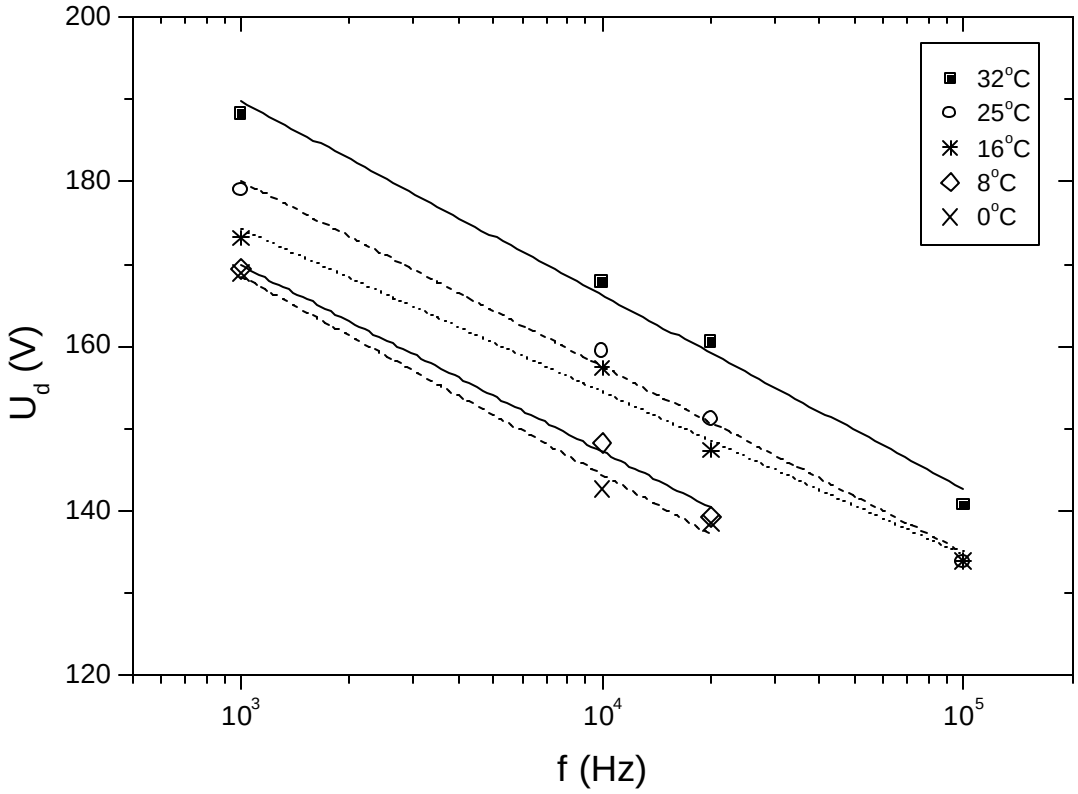


Fig.12

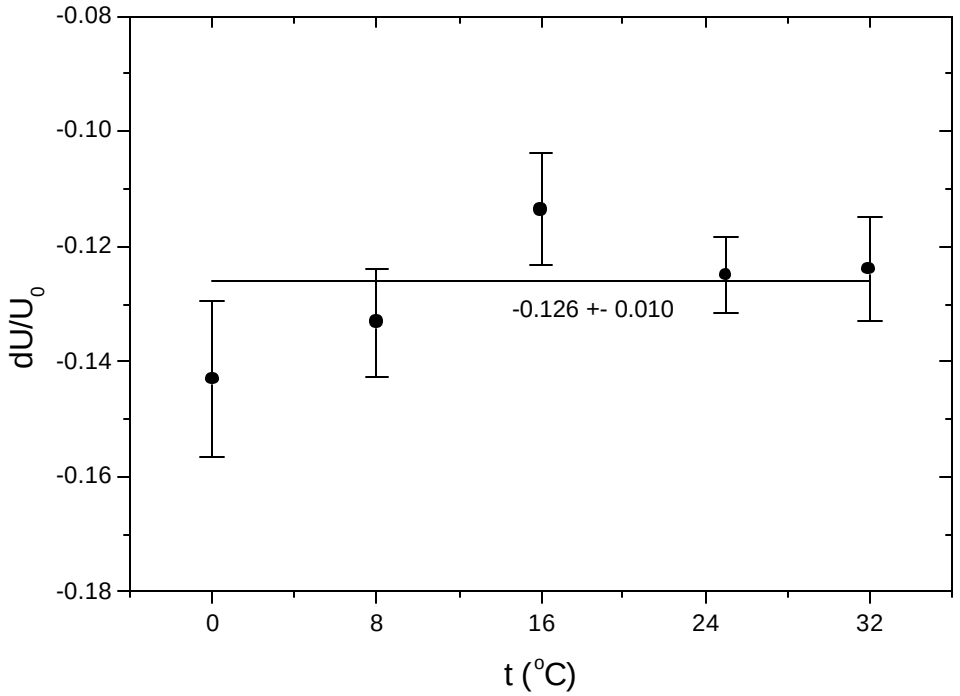


Fig.13

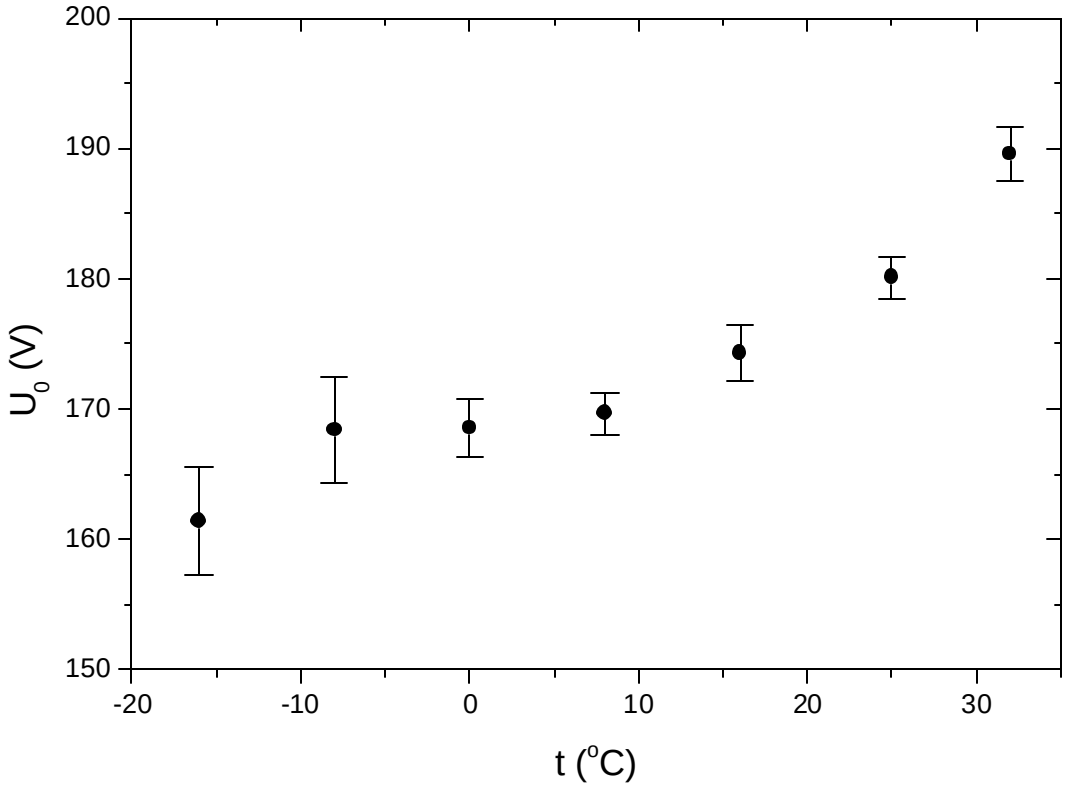


Fig.14

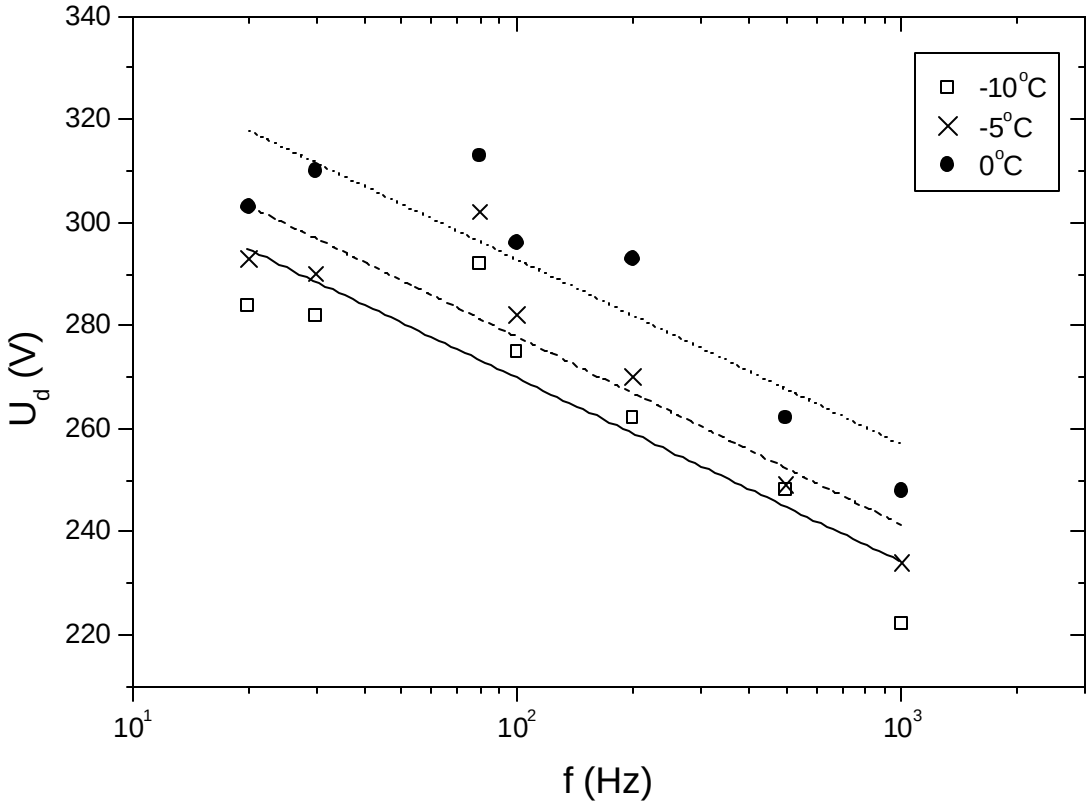


Fig.15

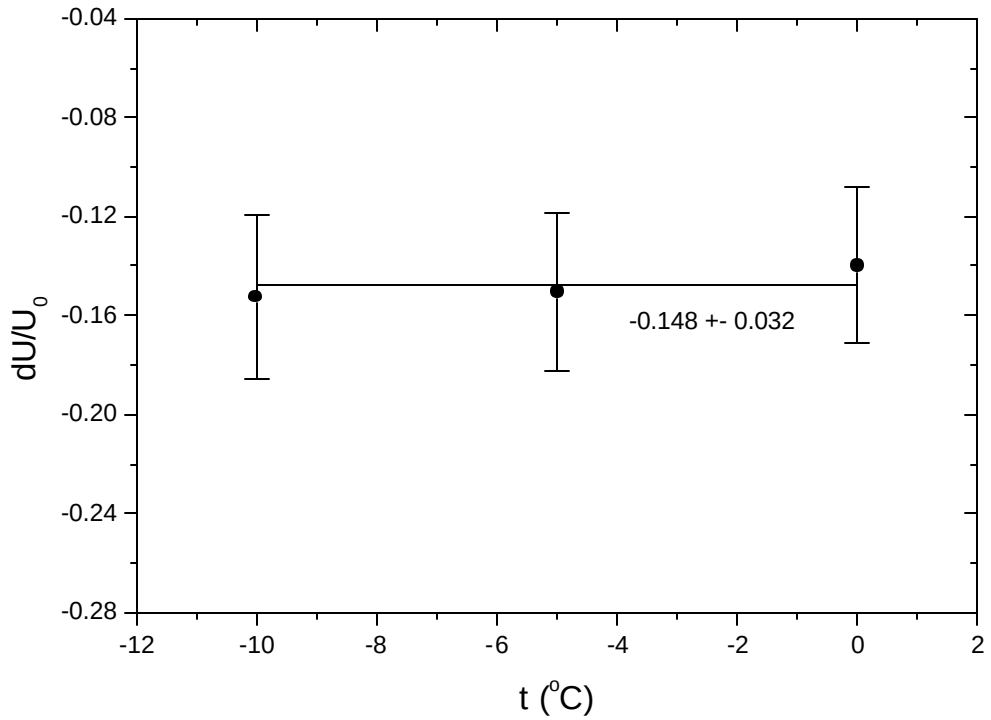


Fig.16

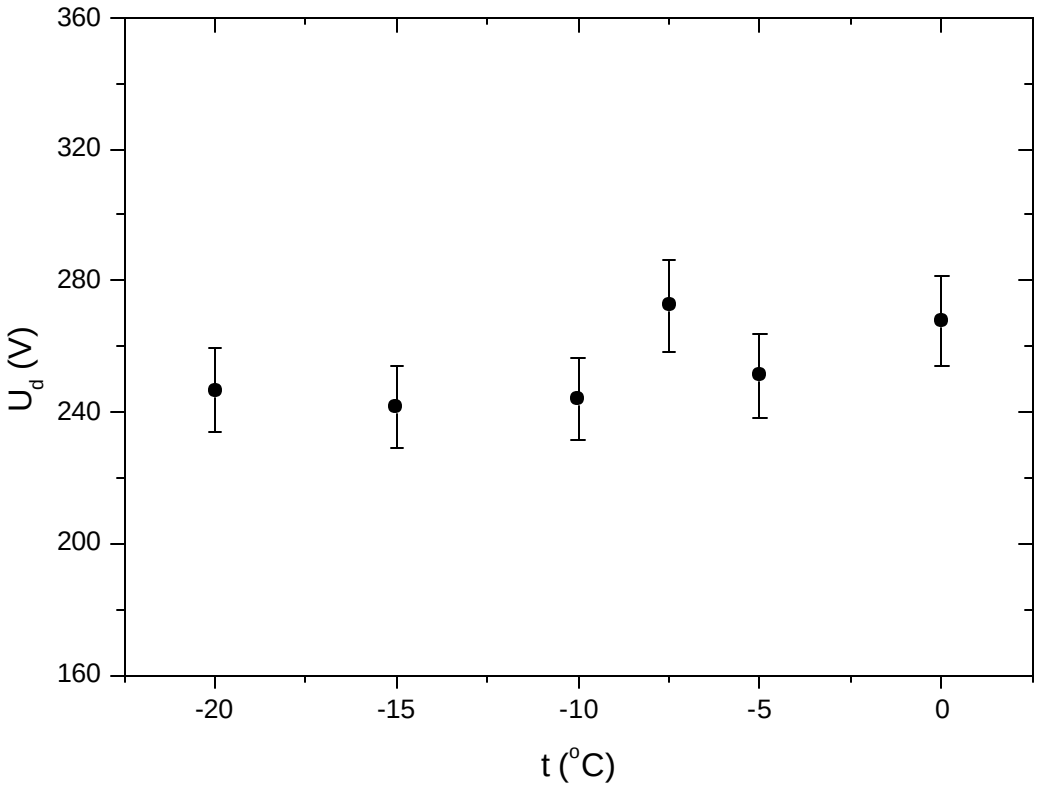


Fig.17

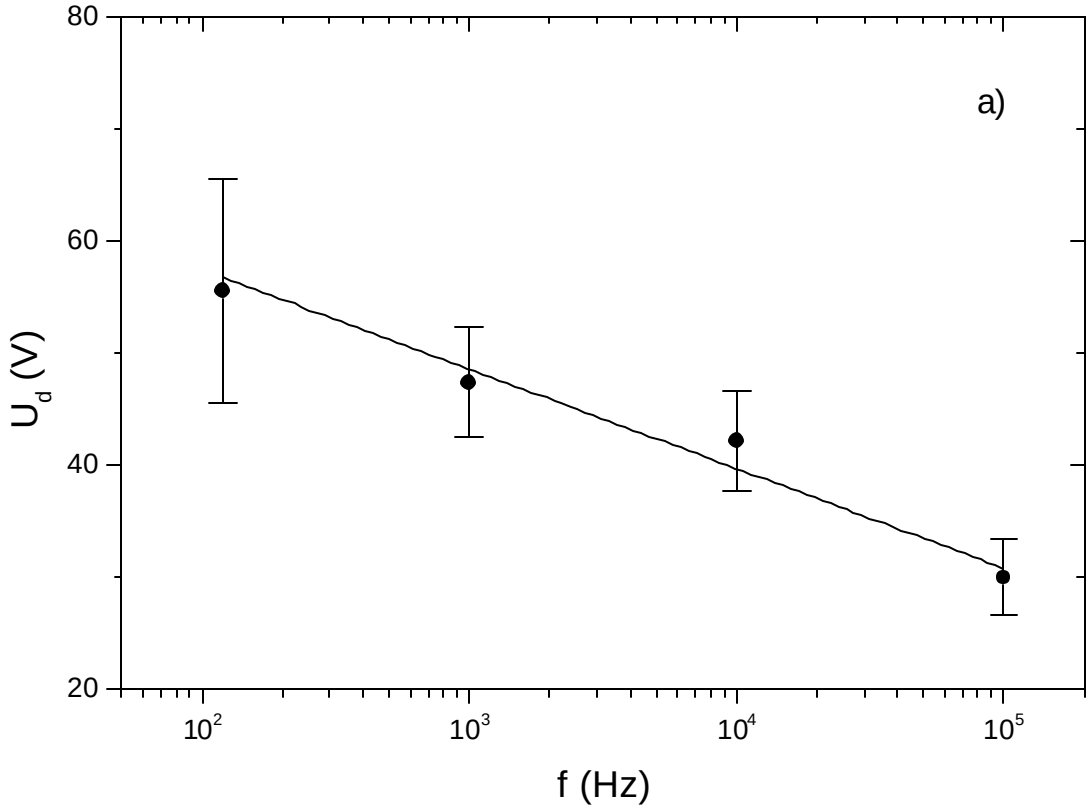


Fig.18a

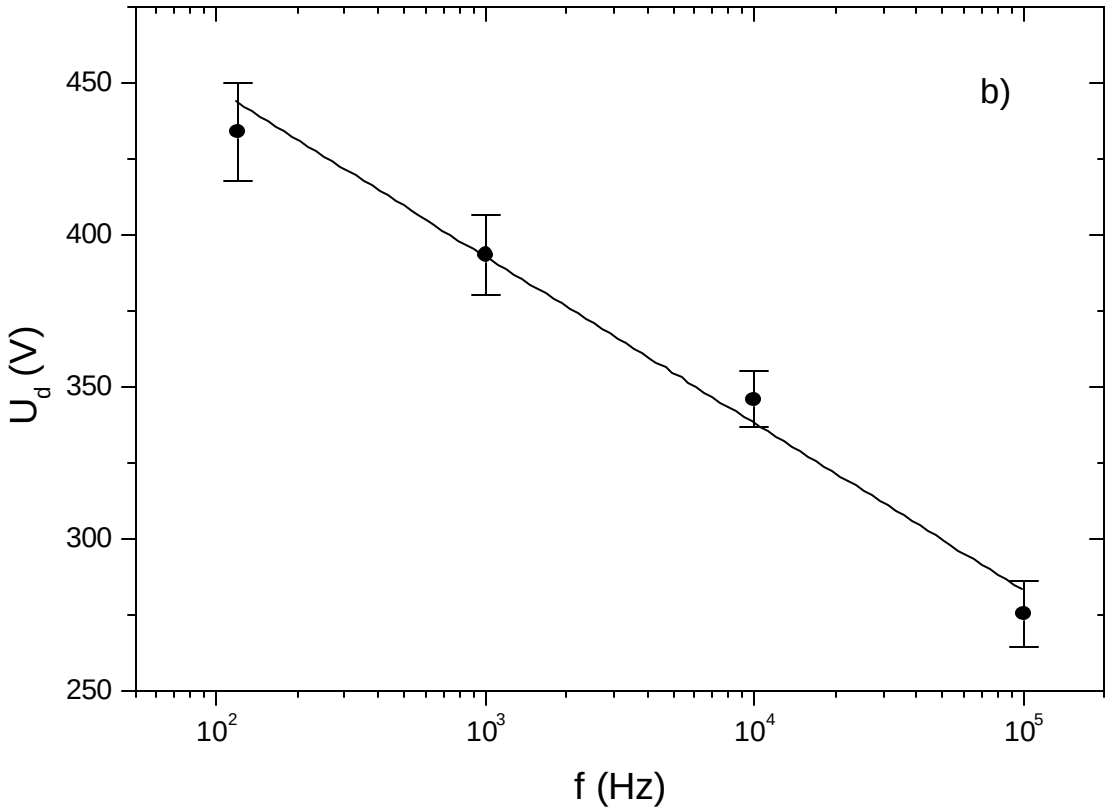


Fig.18b

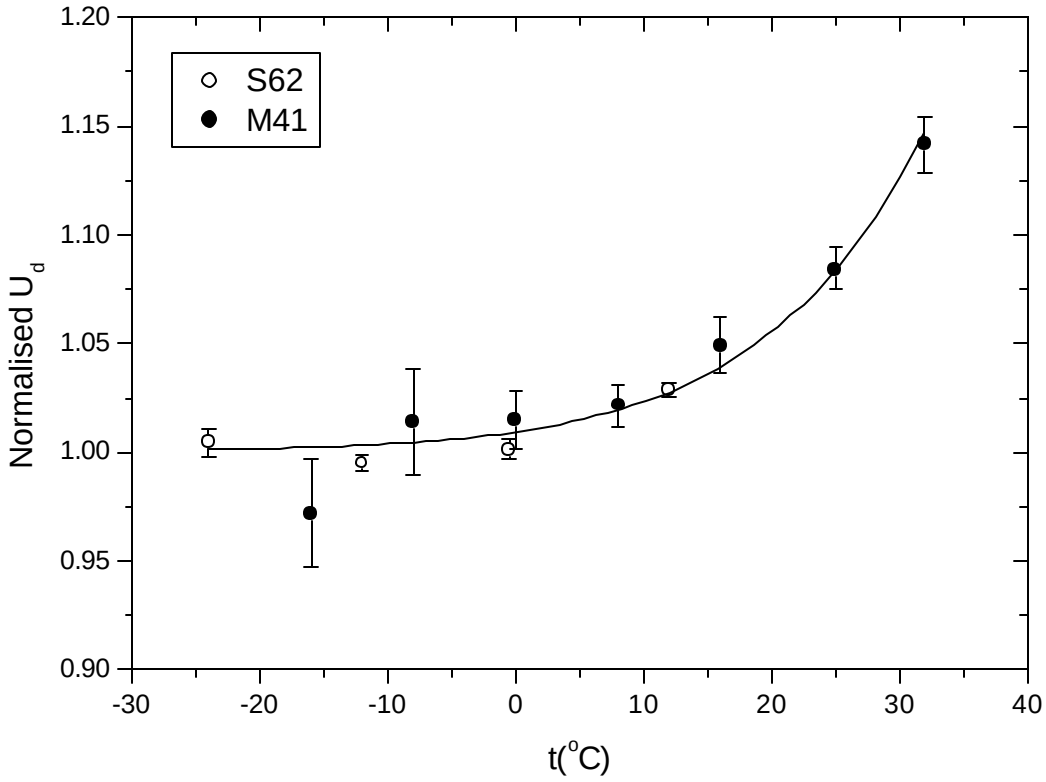
S62
M41
Normalised $U_d$
t($^o$C)
1.20
1.15
1.10
1.05
1.00
0.95
0.90
-30
-20
-10
0
10
20
30
40

Fig.19

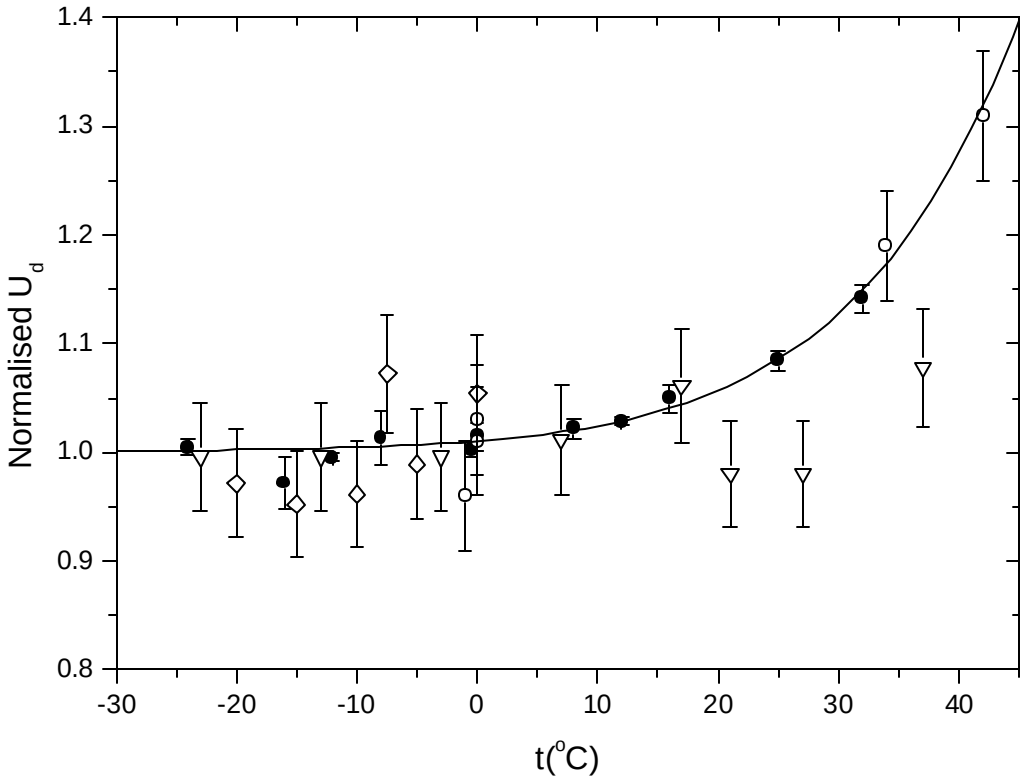


Fig.20

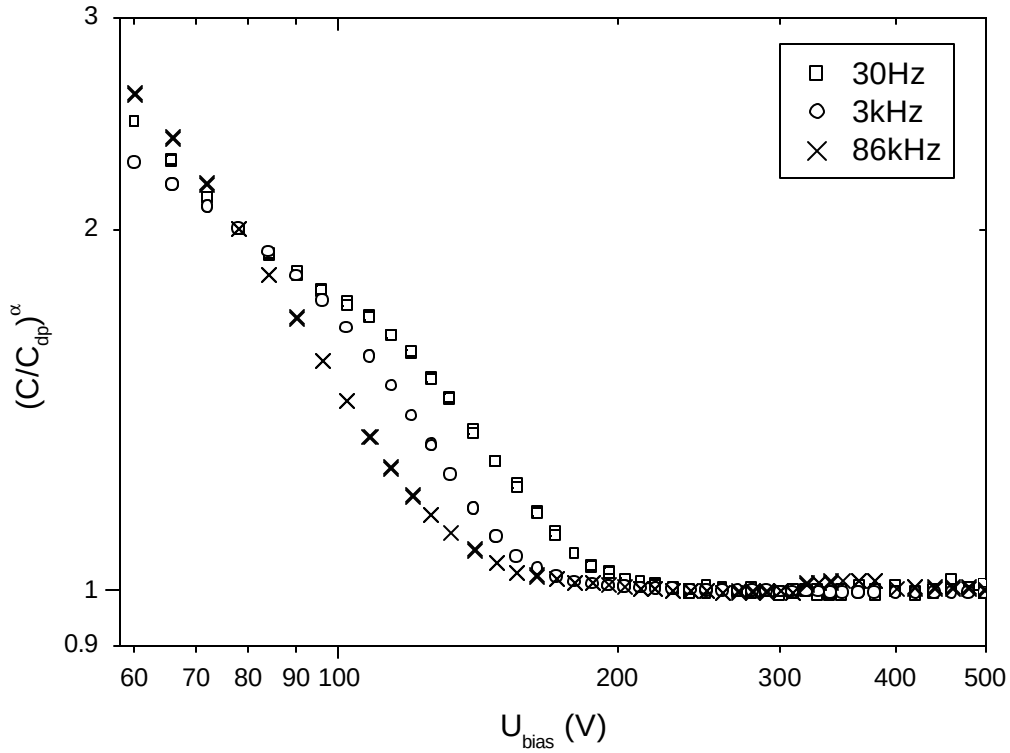
3
2
1
0.9
60
70
80
90
100
200
300
400
500
30Hz
3kHz
86kHz
$(C/C_{dp})^{\alpha}$
$U_{bias}$ (V)

Fig.21

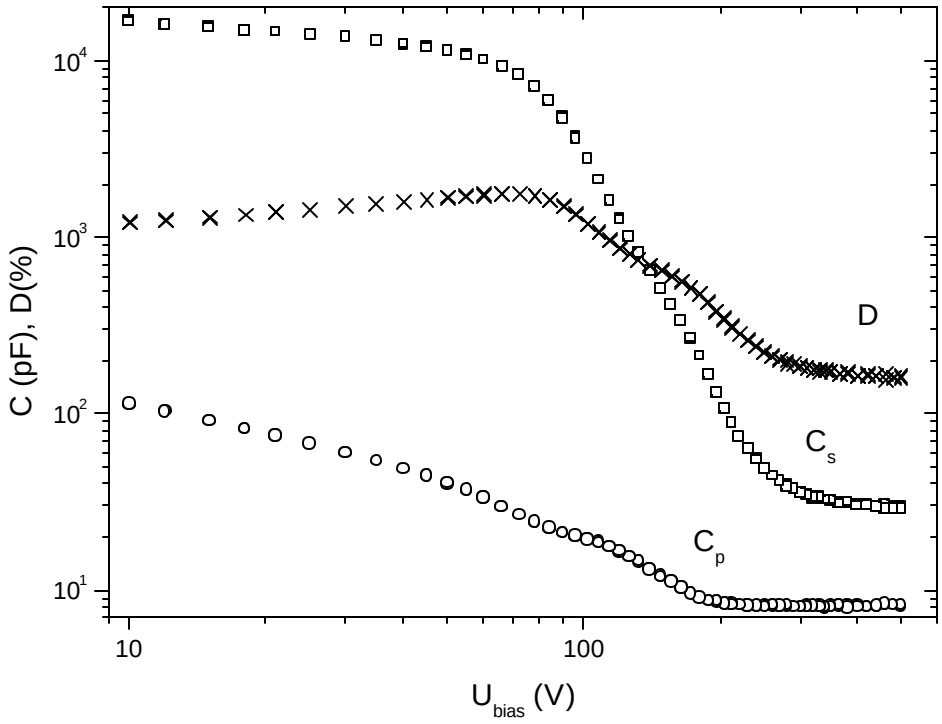


Fig.22